The Nature of Tunneling Pathway and Average Packing Density Models for Protein-Mediated Electron Transfer†

Megan L. Jones, Igor V. Kurnikov,‡ and David N. Beratan*

Departments of Chemistry and Biochemistry, Box 90346, Duke University, Durham, North Carolina 27708-0346

Received: September 4, 2001; In Final Form: December 11, 2001

The last 30 years have witnessed the development of increasingly successful theoretical approaches to predicting how a protein's chemical composition and three-dimensional structure influence its propensity to mediate electron-transfer reactions. Analysis has progressed from uniform-barrier models that neglect atomic detail, to pathway models that incorporate the specific nature of the bonding and the protein fold, to multipathway models that add coherently the contributions of pathways, to methods that average over accessible geometries. Large-scale electronic structure methods remain of somewhat limited use because: the demands of geometry sampling and electronic structure calculation are considerable, especially for slower ET events; qualitative new insights arising from the more intensive analysis have been moderate; and structure−function relations become increasingly difficult to derive from more complex models. For these reasons, simple models remain both useful and popular. The simplest structured-protein models employ tunneling pathway and average packing density analysis. These methods are derived from the same protein physics: electronic interactions decay much more rapidly through-space than through-bond. We show that for the majority of 38 donor−acceptor pairs in 28 proteins with determined X-ray structures, the two models are in qualitative agreement. However, for five of these donor−acceptor pairs**,** the pathway and the average packing density predictions are qualitatively different. The structural reasons for these differences are clear: (1) strong coupling pathways may exist in regions of unremarkable packing density, (2) explicit water molecules added to the X-ray structures can eliminate otherwise costly through-space jumps, (3) strong pathways situated beyond the zone sampled in average packing density analysis can dominate. We suggest that the instances of substantial differences between the two models can be used to probe ET tunneling mechanism. Differences, where they exist, point to specific structural motifs where pathway effects associated with a protein's three-dimensional structure might play a central role in ET kinetics.

I. Introduction

Many electron transfer (ET) reactions within and between proteins occur at donor−acceptor distances well beyond van der Waals contact.[1−8] ET cofactors are not usually sufficiently oxidizing or reducing to exchange electrons with the protein medium itself. As such, ET occurs via weak donor−acceptor mixing facilitated by the protein medium, and the mechanism is generally nonadiabatic with rate given by eq 1:

$$k_{ET} = \frac{2\pi}{\hbar}|H_{DA}|^2(FC) \qquad (1)$$

Here H_{DA} is the coupling matrix element and FC is the Franck−Condon weighted density of states.[5,6] Because biological electron transfer occurs via vibronically coupled electron tunneling,[9] considerable theoretical effort has focused on understanding the mechanism of the protein-assisted tunneling process.[3−23]

Electron transfer kinetic data on native and modified proteins is becoming increasingly available,[24−32] and a number of comparisons between theory and experiment are accessible.[12,26,27,30−32] Recently reported X-ray structures of Ru-modified proteins are removing structural uncertainties associated with the modified proteins.[25,29] Depending on the level of resolution demanded, any given model may, of course, be deemed successful or unsuccessful. The goal of this paper is to compare the physical ingredients of the pathway and average packing-density models, and to make quantitative comparisons of their predictions. From this analysis, we conclude that in most cases the predictions are indistinguishable. However, we identify specific cases where the predictions differ by orders of magnitude. The differences arise quite clearly from the manner in which the two models incorporate and sample details of a protein's three-dimensional structure.

II. Empirical Models for Protein-mediated Coupling

A number of empirical models have been proposed for estimating H_{DA}. The simplest are the square barrier,[9,33,34] tunneling pathway,[10−15] and average packing density models.[32] These three models remain in relatively wide use.[3] Each makes concrete predictions of relative or absolute rates, and the models also connect structure with function. Electronic structure models, based on extended-Hückel or other tight-binding Hamiltonians,[15,16,20,35] self-consistent field methods,[36,37,19] and pseudopotential-based methods[38,39] are also accessible. A simplification intrinsic to the empirical methods is that they are not hypersensitive to geometry. Electronic structure-based methods include the influence of multiple interfering tunneling pathways;

† Part of the special issue "Noboru Mataga Festschrift".

‡ Current address: Department of Chemistry, Northwestern University, Evanston, IL 60208.

10.1021/jp0133743 CCC: $22.00
Published on Web 02/16/2002

these interferences can be strongly geometry dependent (depending on the donor/acceptor energetics, three-dimensional protein structure, and calculational methods). Selection of one (or even several) geometries for coupling analysis can lead to uncharacteristically large or small coupling elements. In fact, fluctuations away from the lowest free energy structure may produce substantial coupling enhancements necessary for biological ET.[40]

Electron tunneling through protein is characterized by a combination of through-bond and through-space interactions. Assuming that the electronic coupling decays across a number of discrete steps in a chain between donor and acceptor, the coupling can be written:

$$|H_{DA}|^2 = A^2\left(\prod_i \epsilon_i\right)^2 \tag{2}$$

If each of these steps i is of equal strength, we may write:

$$\epsilon_i = \bar{\epsilon} \text{ for all steps } i$$

$$|H_{DA}|^2 = A^2\,\bar{\epsilon}^{2N} = A^2 \exp[-\beta R_{DA}]$$

and

$$\beta = -\frac{2N}{R_{DA}} \ln \bar{\epsilon} \tag{3}$$

In purely periodic bridging systems, the assumption of a single average decay parameter for each repeating unit is justified,[41] and the result is rigorously valid in the extreme perturbative limit first described for chemical bridges by McConnell.[42] In aperiodic bridges, one would not generally expect ϵ_i (or β) to adopt universal values, and considerable exploration of these parameters exists in the small-molecule ET literature.[43−46] Typical values of β estimated from families of protein ET rate studies range from 1.0 to 1.5 Å^{-1}.[3,13]

The decay of electronic coupling interactions through bond and through space is qualitatively different. Typical ionization potentials (IPs) associated with protein cofactors are estimated to be ∼5 eV (based on redox potential arguments).[47,48] The electrons of the protein are more tightly bound, with IPs of ∼7−9 eV. The difference between these two IPs introduces an energy barrier for the electron to leave the cofactors. Since this barrier energy is much larger than thermal energies, the electron tunnels from donor to acceptor, and the tunneling barrier height is approximately equal to the difference in the two IPs, ∼ 2 eV. In one-dimensional models, β scales with the square root of this barrier height. A 5 eV (through-space) barrier produces $\beta \sim 2.3$ Å^{-1}. The value resulting from a 2 eV (through-bond) tunneling barrier is ∼1.4 Å^{-1}, and was first noted by Hopfield.[9] Estimating the average β value for proteins requires balancing the through-bond and through-space decays, based on the three-dimensional structure of the protein. Pathway estimates of average decay parameters between 1.1 Å^{-1} (for β-sheets structures) and 1.4 Å^{-1} (for α-helical structures)[10,37] were derived from per bond coupling decay parameter of 0.6 (0.36 decay of H_{DA}^2) and explicit examination of the three-dimensional structure of proteins.

The tunneling pathway model uses experimental data to parametrize the through-bond decay (from saturated hydrocarbon bridged donor−acceptor systems studied by Closs and Miller in the mid-1980s[49]). The experimental distance dependencies indicated $\epsilon_{bond}^2 \sim 0.36$. Initial estimates of $\epsilon_{space}^2 \sim 0.36 \exp[-3.4(R - 2.8\text{ Å})]$ were based on cofactor binding energies of 11.8 eV, larger than expected for physiological cofactors. These large values compensate, to some extent, for unfavorable orbital overlap factors between bonds interacting through space. The through-space exponents of 3.4 Å^{-1} (pathways) and 2.8 Å^{-1} (average packing density) result in rate ratios between the two methods of 7.7 for a 3.4 Å through-space step. Simple estimates suggested pathway decay factors for hydrogen bonds (heteroatom to heteroatom) of about $\epsilon_{H\text{-}bond} \cong \epsilon_{bond}^2$, and these predictions have been supported by experiment.[3]

The pathway model searches proteins for the combination of steps that *maximize* the product of eq 2. Separating into bonded, nonbonded, and hydrogen-bonded steps:

$$|H_{DA}|^2 = A^2\left(\prod_i \epsilon_{bond}(i)\right)^2\left(\prod_j \epsilon_{space}(j)\right)^2\left(\prod_k \epsilon_{H\text{-}bond}(k)\right)^2 \tag{4}$$

As such, the pathway model reflects the large difference in through-bond and through-space electronic propagation.

The average packing density-based tunneling model similarly balances the through-bond and through-space decay of electronic interactions in proteins. The model writes:[32]

$$|H_{DA}|^2 = A^2 \exp\{-[0.9\rho + 2.8(1-\rho)][R_{DA} - 3.6]\}$$

with

$$0 \le \rho \le 1 \quad \text{and} \quad R_{DA} \text{ in ångstroms} \tag{5}$$

Here, the overall average packing density, ρ, rather than the pathway connectivity, defines the coupling. The average packing density is calculated in a region of protein defined by the line segments joining each donor atom to each acceptor atom. Note that the exponential decay of $|H_{DA}|^2$ varies from a minimum value of 0.9 to a maximum of 2.8 Å^{-1} in this model. The parameter ρ is the fraction of sampled space between donor and acceptor cofactor atoms that fall inside the van der Waals radii of the protein atoms, and waters (modeled into the structure using the droplet method of the program Sybyl[32]).

Pathway and average packing density analysis is computationally simple to perform. While the calculations cannot be performed "by hand," they require no more than a few seconds on a modern personal computer.[50] The mathematical isomorphism of the two methods is clearly seen by writing the squared coupling in both models as[51]

$$|H_{DA}|^2 = A^2\,(\epsilon_{space})^{2N_S}(\epsilon_{bond})^{2N_C} \qquad \text{(pathway } \textit{and} \text{ density models)} \tag{6a}$$

and defining the through-bond and through-space tunneling distances accordingly

$$R_{bond} = \rho(R_{DA} - 3.6) \quad \text{and} \quad R_{space} = (1-\rho)(R_{DA} - 3.6) \tag{6b}$$

$$\epsilon_{bond}{}^{2N_C} = \exp[-0.9R_{bond}] \qquad (\textit{density} \text{ model}) \tag{6c}$$

$$\epsilon_{space}{}^{2N_S} = \exp[-2.8R_{space}] \qquad (\textit{density} \text{ model}) \tag{6d}$$

The pathway implementation uses

$$\epsilon_{bond}{}^{2N_C} = (0.6)^{2N_C} \cong \exp[-0.8R_{bond}] \qquad (\textit{pathway} \text{ model, extended chain}) \tag{7a}$$

$$\epsilon_{space}{}^{2N_S} = \exp[-3.4R_{space}] \qquad (\textit{pathway} \text{ model}) \tag{7b}$$

As such, the average packing density and pathway models are *mathematically isomorhpic*, but they differ in (1) the ratio of

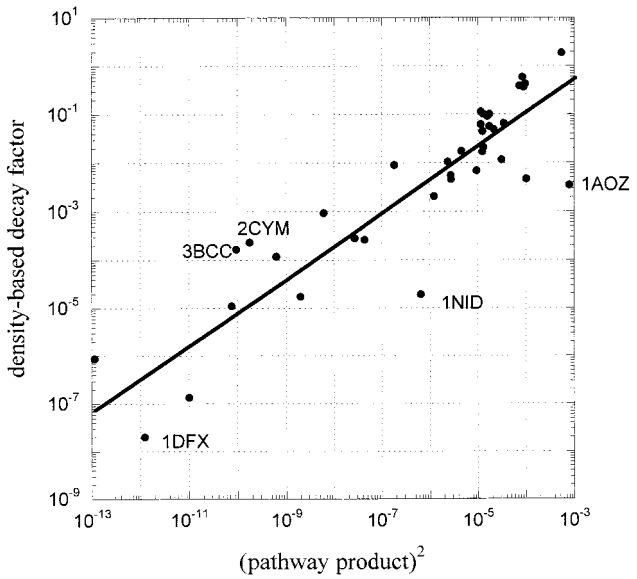

Figure 1. Comparison of relative coupling values for the pathway and average packing density models.[32,53] Pathway values are $\Pi\epsilon_i$ for the strongest paths and the average packing density values are $\exp\{-[0.9\rho + 2.8(1 - \rho)][R_{DA} - 3.6]\}$. The slope of the "best fit" line is 0.7, reflecting the difference between the through-space decay factors in the two models.

the through-bond to through-space decay parameters and (2) the assignment of N_C and N_S (equivalently, R_{bond} and R_{space}), the number of through-bond and through-space steps for the donor−acceptor pair in the protein environment. The average packing density approach assigns N_C and N_S on the basis of the *average* density of atoms in the tube between donor and acceptor, including modeled waters.[32] The standard pathway implementation does not model these waters explicitly (recent data suggest the mediation characteristics of water are intermediate between protein and vacuum[28,52]). The pathway model assigns N_C and N_S on the basis of the single strongest pathway of through-bond and through-space steps linking any pair of donor and acceptor cofactor atoms, without restriction of this pathway to any particular region of space. We next examine the consequences of these two modest differences between models for protein ET rate predictions.

III. Pathway and Density Analysis: A Direct Comparison

The pathway-coupling estimate is based on the single strongest donor−acceptor route while the average density approach is based on the "averaged" intervening medium. Figure 1 compares the pathway with the density-derived squared (relative) couplings for 38 donor−acceptor pairs in 28 proteins whose average density values were determined by Dutton and co-workers.[53] We use the same cofactor delocalization rules as in ref 53.

Figure 1 shows that, despite the difference in parametrization, only 5 of the 38 proteins have order of magnitude differences in their predictions (the slope of the correlation line is discussed in the next section). Those proteins well above the line have a stronger density based coupling, while those below the line have a stronger predicted pathway-based coupling. The proteins with a dramatically larger pathway-based coupling are nitrite reductase (1NID), ascorbate oxidase (1AOZ), and desulfoferrodoxin (1DFX). The proteins with a much greater density-based coupling are the cytochrome bc_1 complex (3BCC) (heme B_L to quinone binding site),[53b] and cytochrome c_3 (2CYM) (heme 108 → heme 110).

Figure 2 shows the strongest pathways for the three systems with the dramatically stronger pathway couplings. The dominant pathway in 1AOZ is 7 steps in length and is nearly linear, including residues 507 and 508 between the copper cofactors. The average packing density is also moderately large, $\rho = 0.86$. In 1NID, the strongest path is also purely covalent, 9 bonds in length; ρ is large too (0.95). This 1NID pathway is arching, and extends beyond the tube sampled in the average density analysis. 1DFX provides an even more dramatic case of an arching but dominantly covalent pathway (19 covalent bonds, one through-space contact). In 1DFX, the dominant pathway extends well beyond the tube sampled in the average packing analysis. The packing density is also moderately large, $\rho = 0.84$. Note that, in all three of these strong-pathway systems, the donor and acceptor cofactors are compact (*not* porphyrin or chlorin macrocycles, for example). As such, the density analysis samples a fairly narrow protein region. Pathways that lie "just beyond" this zone in 1NID and 1DFX are very strong, despite the moderately large packing densities. In summary, pathway-based couplings are much larger than average density-based couplings when an extremely strong pathway exists in an otherwise average region of the protein. The differences in predicted couplings can be particularly large when the donor and acceptor cofactors are especially small in size. In this case, the average medium sampled in the packing model may not be representative of the electron tunneling-mediating medium.

Figure 2 also shows the dominant pathways for the two proteins with ET couplings predicted to be much weaker in the pathway analysis than in the average density-based strategy. Both 3BCC and 2CYM have pathways including two long through-space jumps (4.2 and 6.2 Å in 3BCC; 5.7 and 4.4 Å in 2CYM). Average packing density is indeed lower in both 3BCC ($\rho = 0.61$) and in 2CYM ($\rho = 0.80$), mirroring the weak connectivity found in the pathway analysis. The role of added water appears particularly important in 3BCC. We compute a density value of only 0.53 when water is not added to the structure.

IV. Summary and Discussion

In summary, for all but a few donor−acceptor pairs studied, the differences in the predictions of the average packing density and pathway models are not significant, given the simplicity of the models. Central to both models is the balance between through-bond and through-space coupling decay in protein electron transfer, and this accounts for the similar predictions. In addition, the similarity of the results from the two methods is consistent with the observation that the strongest single pathway is generally a member of a family of many pathways with similar coupling strengths.[15] The spatial range over which the protein packing density is averaged (in the density model) is somewhat arbitrary. As such, it may underestimate the influence on the coupling of strong pathways that exist in otherwise average regions (the cases of 1AOZ or 1NID). Second, it neglects the influence of strong coupling paths that lie beyond the cutoff tubes (as in 1DFX). On the other hand, pathway analysis is limited by its neglect of mediation likely provided by waters not revealed in the X-ray structural data for 3BCC and 2CYM. Both theoretical models ignore explicit multiple-pathway interferences and dynamical fluctuations in couplings,[54−57] although one may argue that both parametrizations include the influence of these effects on the coupling because the parameters are derived from experiment.

Further differences between the pathway and average packing density parametrizations are also easy to probe and to under-

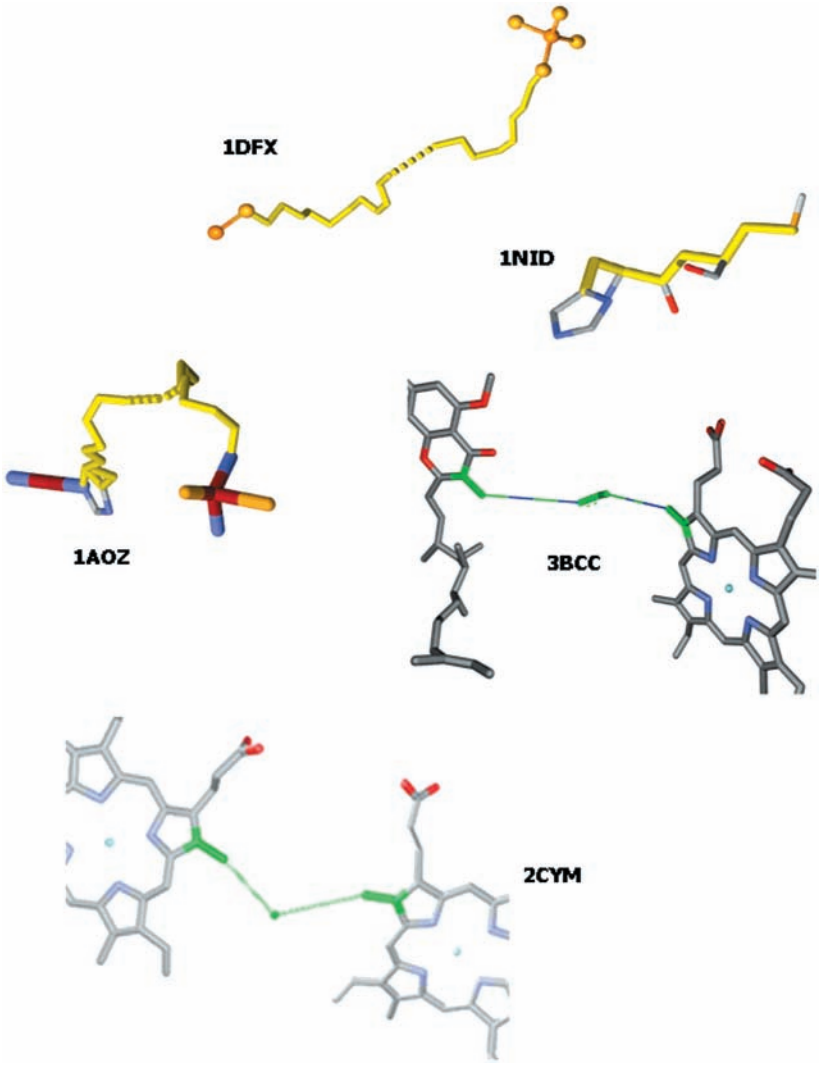

Figure 2. Strongest pathways are shown for three proteins that have much stronger pathway couplings than average density couplings (1AOZ, 1DFX, and 1NID), and for two proteins with much weaker pathway than density-based couplings (3BCC and 2CYM). The 1NID and 1DFX strongest pathways are direct and strong: covalent and hydrogen-bonded steps lie along nearly straight lines from donor to acceptor. The strongest pathway in 1AOZ is also covalent and hydrogen bonded, but lies outside the zone sampled in the packing density model. The weak 3BCC and 2CYM pathways both have two long-distance through-space gaps. Since the packing-density fills these gaps with water ("bonded medium"), the coupling predicted is substantially larger in that model.

stand. Fitting H_{DA}^2 to a single exponential for these 28 proteins yields 1.4 $Å^{-1}$ for the average packing density model (see also ref 32) and 1.6 $Å^{-1}$ for the pathway model. In the log−log plot of Figure 1, therefore, the expected slope derived from the two methods is expected to be 1.4/1.6, or 0.88. This value is approximately the slope of the best-fit line through the dataset in Figure 1.

Nearly all of the structured-protein methods used to analyze ET processes in the last 15 years have attempted to define key amino acids or tunneling zones that mediate couplings. Pathway models,[10] path integrals calculations,[39] extended-Hückel analysis,[17,20] IAL Hamiltonian calculations,[36] tunneling current methods,[16] pathway tube analysis,[14] electronic contact maps,[58,59] importance analysis,[60] worm models,[18] and other semiempirical and ab initio electronic structure approaches[19,24,37,38] assist in defining the role of specific groups that mediate donor−acceptor electronic coupling. More recent calculations have probed dynamical effects on the coupling[54−57] and the potential role of dynamical amplification of ET rates.[40] These methods succeed qualitatively to the extent that they properly balance through-bond and through-space tunneling propagation.[10] The methods agree with each other in most cases. Large differences, where they exist, motivate valuable ET experiments. Moreover, differences between pathway and average-density predictions may indicate evolutionary "wiring" of specific coupling routes.[61] Taken together, these electron-tunneling models provide a powerful arsenal for assessing tunneling mechanism, designing experiments, and estimating long-range donor−acceptor interactions in proteins.

Acknowledgment. We thank Harry Gray and Les Dutton for spirited discussion of these issues. The atomic density analysis data cited in this paper was provided graciously by C.C. Page, C.C. Moser, X. Chen, and P.L. Dutton. This research was supported in part by grant GM48043 from the National Institutes of Health and Grant CHE-9727657 from the National Science Foundation.

References and Notes

(1) Mataga, N.; Kubota, T. *Molecular Interactions and Electronic Spectra*; M. Dekker: New York, 1970.

(2) Bolton, J. R., Mataga, N., McLendon, G., Eds. *Electron Transfer in Inorganic, Organic, and Biological Systems*; American Chemical Society: Washington, D.C., 1991.

(3) Bendall, D. S. *Protein Electron Transfer*; Bios Scientific Publishers: Oxford, 1996.
(4) Canters, G. W., Vijgenboom, E., Eds. *Biological Electron-Transfer Chains: Genetics, Composition and Mode of Operation*; Kluwer Academic Publishers: Dordrecht, 1998.
(5) Balzani, V., Ed. *Electron-Transfer Reactions*; Wiley-VCH: Weinheim, 2001; Vols. 1−5.
(6) *Adv. Chem. Phys*. **1999**, *106* and *107*.
(7) Bertini, I.; Gray, H. B.; Lippard, S. J.; Valentine, J. S. *Bioinorganic Chemistry*; University Science Books: Mill Valley, CA, 1994.
(8) Lippard, S. J.; Berg, J. M. *Principles of Bioinorganic Chemistry*; University Science Books: Mill Valley, CA, 1994.
(9) Hopfield, J. J. *Proc. Natl. Acad. Sci. U.S.A.* **1974**, *71*, 3840.
(10) Beratan, D. N.; Betts, J. N.; Onuchic, J. N. *Science* **1991**, *252*, 1285.
(11) Beratan, D. N.; Betts, J. N.; Onuchic, J. N. *J. Phys. Chem*. **1992**, *96*, 2852.
(12) Onuchic, J. N.; Beratan, D. N.; Winkler, J. R.; Gray, H. B. *Annu. Rev. Biophys. Biomol. Struct.* **1992**, *21*, 349.
(13) Skourtis, S. S.; Beratan, D. N. *Adv. Chem. Phys*. **1999**, *106*, 377.
(14) Regan, J. J.; Onuchic, J. N. *Adv. Chem. Phys*. **1999**, *107*, 497.
(15) Regan, J. J.; Risser, S. M.; Beratan, D. N.; Onuchic, J. N. *J. Phys. Chem.* **1993**, *97*, 13083.
(16) Stuchebrukhov, A. A. *J. Chem. Phys.* **1996**, *104*, 8424.
(17) Okada, A.; Kakitani, T.; Inoue, J. *J. Phys. Chem.* **1995**, *99*, 2946.
(18) Kawatsu, T.; Kakitani, T.; Yamato, Y. *J. Phys. Chem. B* **2001**, *105*, 4424.
(19) Ivashin, N.; Kallebring, B.; Larsson, S.; Hansson, O. *J. Phys. Chem. B* **1998**, *102*, 5017.
(20) Siddarth, P.; Marcus, R. A. *J. Phys. Chem.* **1993**, *97*, 13078.
(21) Lopez-Castillo, J.-M.; Filali-Mouhim, A.; Jay-Gerin, J. P. *J. Phys. Chem*. **1993**, *97*, 9266.
(22) Bicout, D. J.; Field, M. *J. Phys. Chem.* **1995**, *99*, 12661.
(23) Gruschus, J. M.; Kuki, A. *J. Phys. Chem. B* **1999**, *103*, 11407.
(24) Babini, E.; Bertini, I.; Borsari, M.; Capozzi, F.; Luchinat, C.; Zhang, X.-Y.; Moura, G. L. C.; Kurnikov, I. V.; Beratan, D. N.; Ponce, A.; DiBilio, A. J.; Winkler, J. R.; Gray, H. B. *J. Am. Chem. Soc.* **2000**, *122*, 4532.
(25) Tezcan, F. A.; Crane, B. R.; Winkler, J. R.; Gray, H. B. *Proc. Natl. Acad. Sci. U.S.A.* **2001**, *98*, 5002.
(26) Gray, H. B.; Winkler, J. R. *Annu. Rev. Biochem.* **1996**, *65*, 537.
(27) Winkler, J. R. *Curr. Op. Chem. Biol*. **2000**, *4*, 192.
(28) Ponce, A.; Gray, H. B.; Winkler, J. R. *J. Am. Chem. Soc*. **2000**, *122*, 8187.
(29) Di Bilio, A. J.; Crane, B. R.; Wehbi, W. A.; Kiser, C. N.; Abu-Omar, M. M.; Carlos, R. M.; Richards, J. H.; Winkler, J. R.; Gray, H. B. *J. Am. Chem. Soc.* **2001**, *123*, 3181.
(30) Winkler, J. R.; Di Bilio, A. J.; Farrow, N. A.; Richards, J. H.; Gray, H. B. *Pure Appl. Chem.* **1999**, *71*, 1753.
(31) Beratan, D. N.; Skourtis, S. S. *Curr. Opin. Chem. Biol*. **1998**, *2*, 235.
(32) Page, C. C.; Moser, C. C.; Chen, X.; Dutton, P. L. *Nature* **1999**, *402*, 47.
(33) Jortner, J. *J. Chem. Phys.* **1976**, *64*, *4860*.
(34) Moser, C. C.; Keske, J. M.; Warncke, K.; Farid, R. S.; Dutton, P. L. *Nature* **1992**, *355*, 796.
(35) Gruschus, J. M.; Kuki, A. *J. Phys. Chem. B* **1999**, *103*, 11407.
(36) Zhang, L. Y.; Friesner, R. A. *Proc. Natl. Acad. Sci. U.S.A.* **1998**, *95*, 13603.
(37) Kurnikov, I. V.; Beratan, D. N. *J. Chem. Phys*. **1996**, *105*, 9561.
(38) Sneddon, S. F.; Morgan, R. S.; Brooks, C. L. *J. Phys. Chem*. **1989**, *93*, 8115.
(39) Kuki, A.; Wolynes, P. G. *Science* **1987**, *236*, 1647.
(40) Balabin, I.; Onuchic, J. N. *Science* **2000**, *290*, 114.
(41) Beratan, D. N.; Hopfield, J. J. *J. Am. Chem. Soc.* **1984**, *106*, 1584.
(42) McConnell, H. M. *J. Chem. Phys*. **1961**, *35*, 508.
(43) Onuchic, J. N.; Beratan, D. N. *J. Am. Chem. Soc*. **1987**, *109*, 6771.
(44) Jordan, K. D.; Paddon-Row, M. N. *Chem. Rev.* **1992**, *92*, 395.
(45) Newton, M. D. *Chem. Rev.* **1991**, *91*, 767−792.
(46) Paulson, B. P.; Curtiss, L. A.; Bal, B.; Closs, G. L.; Miller, J. R. *J. Am. Chem. Soc.* **1996**, *118*, 378.
(47) Cramer, W. A.; Knaff, D. B. *Energy Transduction in Biological Membranes*; Springer-Verlag: New York, 1990.
(48) Bard, A. J.; Falkner, L. R. *Electrochemical Methods*, 2nd ed.; Wiley: New York, 2001.
(49) Closs, G. L.; Miller, J. R. *Science* **1988**, *240*, 440.
(50) Kurnikov, I. V. *Harlem*, http://www.kurnikov.org/.
(51) Beratan, D. N.; Skourtis, S. S. In *Biological Electron-Transfer Chains: Genetics, Composition and Mode of Operation*; Canters, G. W., Vijgenboom, E., Eds.; Kluwer: Dordrecht, The Netherlands, 1998; pp 9−27.
(52) Miller, N. E.; Wander, M. C.; Cave, R. J. *J. Phys. Chem. A* **1999**, *103*, 1084.
(53) (a) Dutton, P. L. 2001. Personal communication. We have analyzed most of the proteins taken in the dataset of ref 32, specifically: aldehyde ferredoxin oxidoreductase (1aor), aldehyde oxidoreductase (1alo), ascorbate oxidase (1aoz), copper amine oxidase (1ksi), cytochrome bc_1 complex (3bcc), cytochrome *c* peroxidase (2pcc), cytochrome c_3 (2cym), cytochrome c_4 (1etp), cytochrome cd_1/nitrite reductase (1aof), desulphoferrodoxin (1dfx), ferredoxin (1dur), flavocytochrome b_2 (1fcb), flavocytochrome *c*/sulphide dehydrogenase (1fcd), formate dehydrogenase (1dfi), hydroxylamine oxidoreductase (1fgh), iron-only hydrogenase (1feh), lignin peroxidase (1b80), NADH/cytochrome P-450 reductase (1amo), Ni−Fe hydrogenase monooxygenase (1phm), photosynthetic reaction center from *Rp. Viridis* (1prc), phthalate dioxygenase reductase (2pia), quinone reductase (1qrd), ribonucleotide reductase R2 subunit (1rib), sulphite oxidase (1sox), and trimethylamine dehydrogenase (2tmd). (b) Note that the results for 3bcc involve nonphysiological species in the cofactor binding sites.
(54) Skourtis, S. S.; Beratan, D. N. In *Electron-Transfer Reactions*; Balzani, V., Ed.; Wiley-VCH: Weinheim, 2001; Vol. 1, pp 109−125.
(55) Wolfgang, J.; Risser, S. M.; Priyadarshy, S.; Beratan, D. N. *J. Phys. Chem. B* **1997**, *101*, 2987.
(56) Kurnikov, I. V.; Zusman, L. D.; Kurnikova, M.; Farid, R.; Beratan, D. N. *J. Am. Chem. Soc*. **1997**, *119*, 5690.
(57) Daizadeh, I.; Gehlen, J. N.; Stuchebrukhov, A. A. *Proc. Natl. Acad. Sci. U.S.A.* **1997**, *94*, 3703.
(58) Skourtis, S. S.; Beratan, D. N. *J. Phys. Chem. B* **1997** *101*, 1215.
(59) Skourtis, S. S.; Beratan, D. N. *JBIC* **1997**, *2*, 378.
(60) Skourtis, S. S.; Regan, J. J.; Onuchic, J. N. *J. Phys. Chem*. **1994**, *98*, 3379.
(61) Ramirez, B. E.; Malmstrom, B. G.; Winkler, J. R.; Gray, H. B. *Proc. Natl. Acad. Sci. U.S.A.* **1995**, *92*, 11949.